

INVESTIGATIONS OF POLYMER FOULING ON HEATED AND COOLED SURFACES

J.C. Kuschnerow, S. Dorn, H. Föste, W. Augustin* and S. Scholl

Technische Universität Braunschweig, Institute for Chemical and Thermal Process Engineering,
Langer Kamp 7, 38106 Braunschweig, Germany, w.augustin@tu-bs.de

ABSTRACT

Polymerizations and polymer processing are among the most important applications in the chemical industry. This study presents an ongoing work and deals with the fouling behavior of an ethylene-vinylacetate-copolymer on different surfaces with varied process parameters. Experiments were performed in a 2 L batch vessel where stainless steel plates were immersed in the dispersion and heated electrically. The thermal fouling resistance was determined by measuring the change of the heat flux caused by the fouling layer. Furthermore, the weight and the structure of the fouling layer were investigated. The temperature of the polymer dispersion, the heat flux density, the material and coating of the surface and the concentration of polymer in the dispersion had been varied. The thermal fouling resistance generally increases with higher heat flux densities and with higher polymer concentrations. The temperature influence of the dispersion on the thermal fouling resistance is depending on the configuration. Electropolished and coated surfaces deliver significant mitigation of polymer fouling behavior. The lowest range of values for thermal fouling resistance were obtained for SICAN and electropolished SICAN surfaces.

INTRODUCTION

Fouling in heat exchangers is a scientific field in industry and academia which is of a large interest. The types of fouling processes [Epstein, 1983] and its impact on industrialized economies [Müller Steinhagen, 2006] has been described. The present study deals with a type of organic fouling. Until now, organic fouling was described in most cases in the context of biofouling [Bott, 1995][Characklis et. al., 1991][Melo, Bott, 1997], and food processing. The most prominent example of investigations of fouling in food processing is milk fouling [Changani et. al., 1997]. The present study covers polymer materials.

As in other technical fields, fouling leads to a series of disadvantages in polymer processing. Most polymerizations are running exothermal, so the reactor has to be cooled during the reaction. Furthermore, the polymer has to be cooled down from reaction temperature after leaving the reactor. In polymer processing, polymer materials have to be transported, mixed with other components e.g. dyes, molten ore pumped as polymer dispersions. In those process

steps the polymer material has to be heated. In all of these steps such as heating or cooling, pumping through pipes or stirring in vessels, fouling can occur. This, for example, deteriorates the performance of heat exchangers and decreases the diameters of pipes. Parts of the fouling layer which detach from the surface can form an undesired impurity in the polymer end product. Therefore, there is a strong demand to understand polymer fouling and find technical solutions to reduce fouling.

The main objective of this study is the identification of the main parameters which are influencing the thermal fouling resistance.

EXPERIMENTAL SET-UP

Polymer fouling experiments are currently performed with a vinyl acetate, ethylene copolymer dispersion (VINNAPAS®LL6120, see Fig. 1) provided by Wacker Chemie AG, Germany. The dispersion is stabilized by polyols.

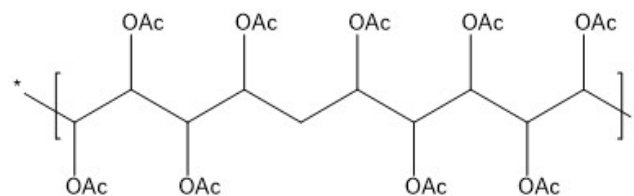


Fig. 1: Structure of VINNAPAS®LL6120

Fouling experiments were performed in a 2 L batch vessel, see Fig. 2, which was held at a constant temperature level. The liquid in the vessel was stirred at a stirring speed of 60 rpm. Two steel plates were mounted on two sides of a heating element with thermocouples fixed directly underneath the plates, thus, two fouling curves were determined in one experiment, see Fig. 6. The plates were heated electrically and a defined heating power could be imposed.

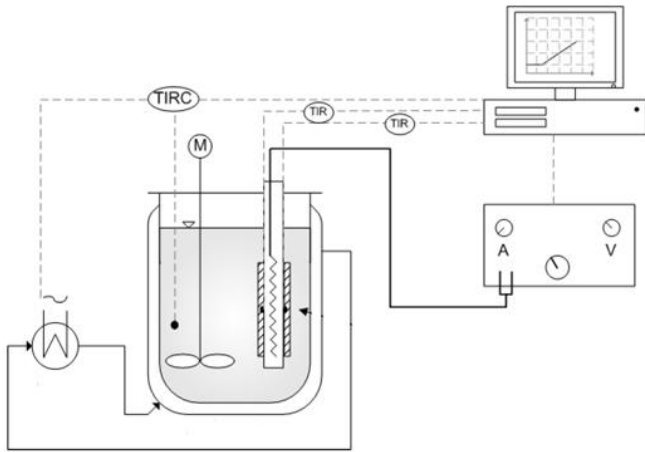


Fig. 2: Test rig for batch fouling experiments [Geddert 2009].

The temperatures were measured and recorded online. Due to a growing fouling layer the thermal fouling resistance increases and can be determined by the recorded temperature $T(t)$, the initial temperature $T(t=0s)$ and the heat flux density, see Eq. 1. Fouling curves deliver the induction time and the thermal fouling resistance as results. Furthermore, the mass of the fouling layers were determined and pictures were taken with a digital microscope and a scanning electron microscope (SEM). Therefore, the sample plates were taken from the test rig with the fouling layer, so the layer was not affected mechanically. With these photos, it is possible to determine the diameter and the height of the craters, which are characteristic for the structure of the fouling layer.

$$R_f(t) = \frac{1}{k(t)} - \frac{1}{k_0}$$

In the experiments, four parameters were varied, the heat flux density, the temperature of the polymer dispersion, the concentration of polymer in the dispersion and the surface material of the sample plates. The temperature was varied from 40 to 70 °C, the heat flux density from 1.7 to 8.5 kW/m² and the concentration from 7.2 to 30 wt-%. As samples plates of stainless steel (type: 1.4301) with technical roughness and electropolished stainless steel was used. Furthermore, stainless steel plates were covered with four different coatings, such as Diamond-Like-Carbon (DLC), a three dimensional but amorphous structure of carbon atoms, SICAN, SICON and enamel. SICAN is similar to a DLC structure, but 20 % of the carbon atoms are replaced by silicon. SICON is similar to SICAN, but contains oxygen atoms additionally. Detail information about these coatings and surfaces are available in [Geddert, 2007]. Electropolished plates with these coatings are indicated as DLC-EP, SICON-EP or SICAN-EP. These steel plates were at first electropolished and then coated. As the thickness of the coating is 3 µm, it does not affect the heat transfer and the roughness of the surface.

The experiments with cooled sample plates were performed in a similar vessel which contains 2.5 L of polymer dispersion. It can also be held on a defined temperature level. Bulk temperatures were set at 50 °C and 70 °C. The plates are fixed on the copper surface of a cooling apparatus with a Peltier element, see Fig. 3. The Peltier element has a cooled surface area of 40 mm x 80 mm, which is equivalent to two sample plates. Two thermocouples are mounted into the copper surface to determine the heat flux. A cooling performance of roughly 90 W could be achieved under operational conditions. The apparatus was specially constructed by Kammrath&Weiss GmbH, Germany, for these studies.

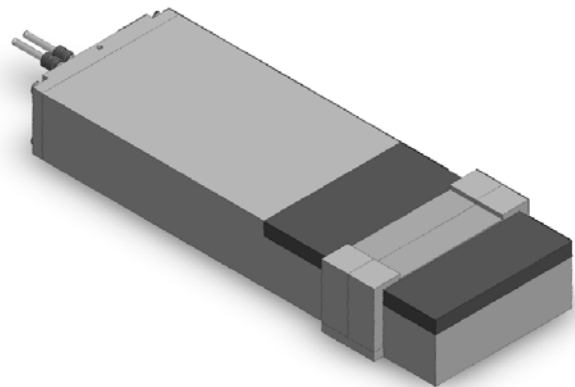


Fig. 3: Design of the Peltier element. The dark part is the copper part which contains the heat transfer unit. Two stainless steel plates are clamped on the apparatus.

RESULTS AND DISCUSSION

Fig. 4 shows typical fouling curves in dependency of the heat flux. In the example, which is shown here, SICAN coated plates were used. It is characteristic for all the experiments performed in this study that there is no induction time. In most cases, the final thermal fouling resistance is reached after a few minutes. In the entire study, the values of the thermal fouling resistance are between 2 and 10 x 10⁻⁴ m²K/W. These figures are in the typical range of fouling behavior for organic fouling [VDI WA, 2006]. In contrast to this, Fig. 5 shows the thermal fouling resistance of the polymer dispersion on electropolished stainless steel. As for plates with technical roughness, significant fouling starts immediately after a few minutes and reaches a comparable level. During this experiment, the thermal fouling resistance fluctuates, which could be explained with parts of the fouling layer detaching from the plate again. Due to the opaque white color of the dispersion, this effect could not be observed visually.

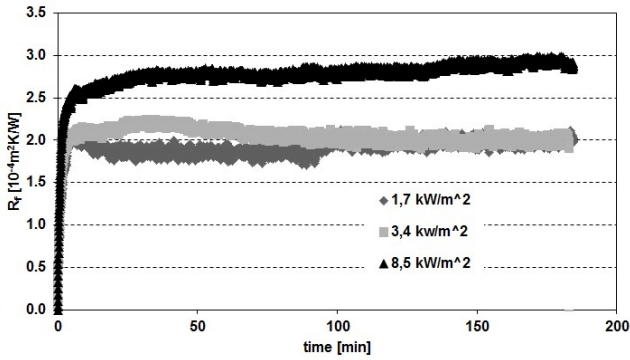


Fig. 4: Fouling curves of experiments with VINNAPAS® LL6120 ($T_f = 50 \text{ }^\circ\text{C}$, $c_{\text{polymer}} = 7,2 \text{ } \%$) on SICAN coated steel.

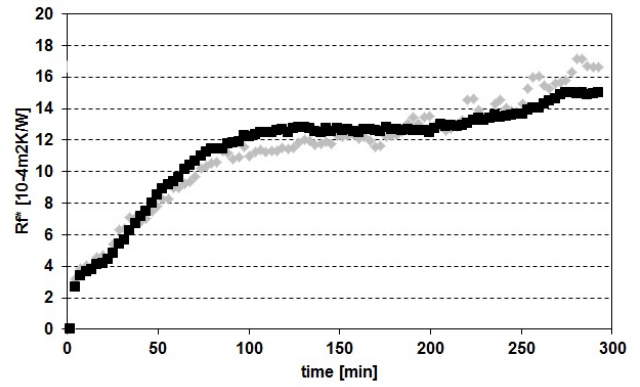


Fig. 6: Fouling curves of experiments with VINNAPAS® LL6120 ($T_f = 46,1 \text{ }^\circ\text{C}$, $c_{\text{polymer}} = 34,9 \text{ } \%$, heat flux density = $3,1 \text{ kW/m}^2$) on enamel coated steel.

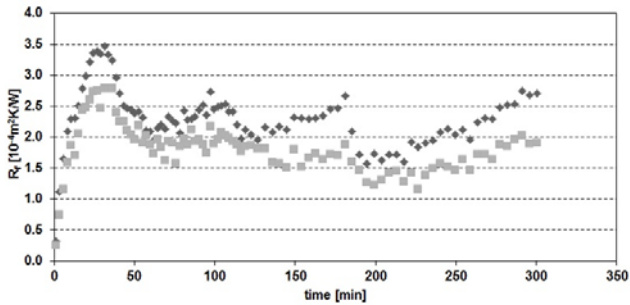


Fig. 5: Fouling curves of experiments with VINNAPAS® LL6120 ($T_f = 63,9 \text{ }^\circ\text{C}$, $c_{\text{polymer}} = 9,2 \text{ } \%$, heat flux density = $3,1 \text{ kW/m}^2$) on electropolished steel.

Figure 6 depicts a fouling curve of an experiment with an enamel surface. As in this example, the thermal fouling resistance is roughly an order of magnitude higher than typical values for the other surfaces in this study. Hence, it is most likely that enamel coatings are not suitable to mitigate polymer fouling.

The dependence of the thermal fouling resistance on the heat flux density on the surface is illustrated in Figure 7 for non electropolished plates and in Figure 8 for electropolished plates. In most cases, higher heat flux densities result in higher thermal fouling resistances. This trend has two interesting exceptions. There is no significant influence on the thermal fouling resistance on SICAN coated plates. For electropolished steel plates, the thermal fouling resistance decreases for the highest values of heat flux density within the investigated range. This fits to all coatings on electropolished surfaces. Values of thermal fouling resistances presented in the following figures are reproducible within a range of 15 %, while the mass of fouling layers can have deviations up to 40 %.

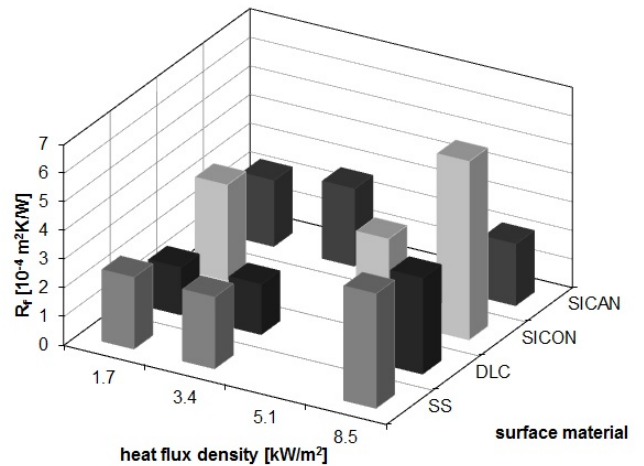


Fig. 7: Influence of the heat flux density on the thermal fouling resistance for non-electropolished surfaces. ($c_p = 11,86\%$; $T_f = 55^\circ\text{C}$ for SICON and $c_p = 7,17\%$; $T_f = 70^\circ\text{C}$ for SS, DLC, SICAN).

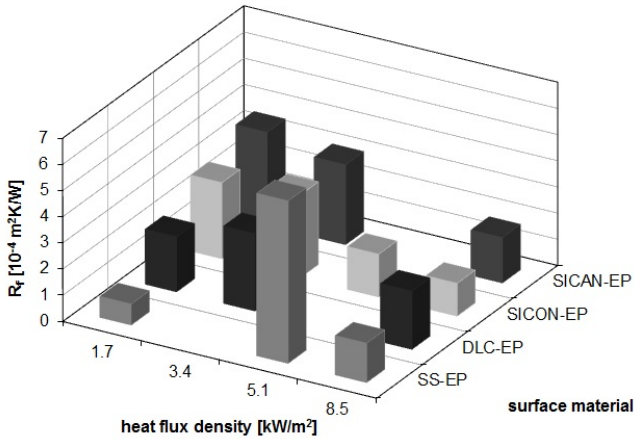


Fig. 8: Influence of the heat flux density on the thermal fouling resistance for electropolished surfaces. ($c_p = 11.86\%$; $T_F = 55^\circ\text{C}$ for SS-EP and $c_p = 7.17\%$; $T_F = 50^\circ\text{C}$ for DLC-EP, SICON-EP, SICAN-EP).

Figures 9 and 10 show the influence of the fluid temperature on the thermal fouling resistance. This operational parameter has the weakest influence on fouling behavior. There are exceptions for SICON® and electropolished steel.

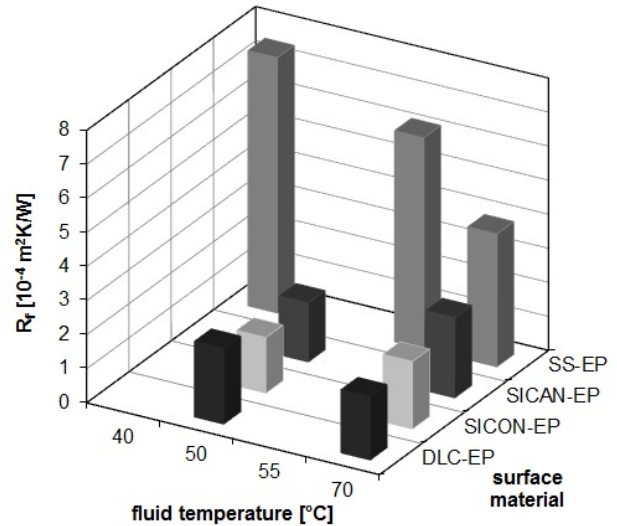


Fig. 10: Influence of the fluid temperature on the thermal fouling resistance for electropolished surfaces. ($c_p = 7.17\%$; $dq/dt = 1.7\text{kW/m}^2$ for SS-EP, $c_p = 7.17\%$; $dq/dt = 5.1\text{kW/m}^2$ for SICON-EP and $c_p = 7.17\%$; $dq/dt = 8.4\text{kW/m}^2$ for DLC-EP, SICAN-EP).

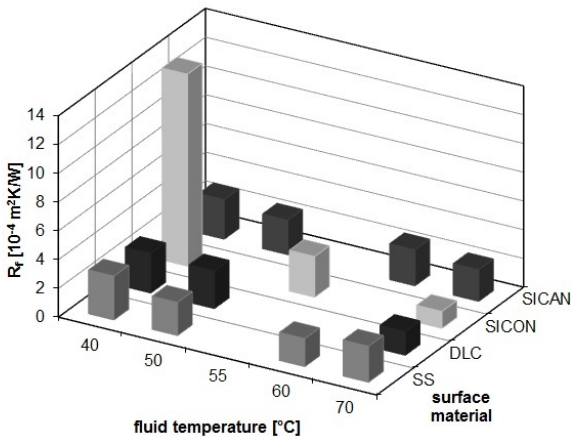


Fig. 9: Influence of the fluid temperature on the thermal fouling resistance for non-electropolished surfaces. ($c_p = 7.17\%$; $dq/dt = 1.7\text{kW/m}^2$ for SICON and $c_p = 11.86\%$; $dq/dt = 5.1\text{kW/m}^2$ for SS, DLC, SICAN).

The dependence of fouling behavior from the concentration of polymer is shown in Figures 11 and 12. As it was expected, higher concentrations of polymer lead to a higher fouling tendency. This trend is quite extreme for the highest concentrations on electropolished surfaces. On non electropolished surfaces, R_f^* values start to increase generally at higher concentrations of polymer. Once again, there are no significant changes of R_f^* for SICAN coated sample plates.

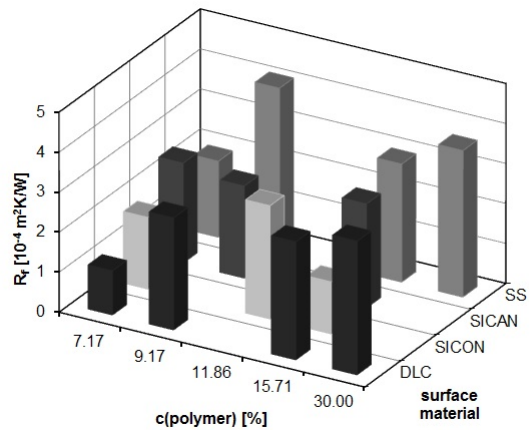


Fig. 11: Influence of the concentration of polymer on the thermal fouling resistance for non-electropolished surfaces. ($T_F = 50^\circ\text{C}$; $dq/dt = 3.4\text{kW/m}^2$ for SICON and $T_F = 55^\circ\text{C}$; $dq/dt = 5.1\text{kW/m}^2$ for SS, DLC, SICAN).

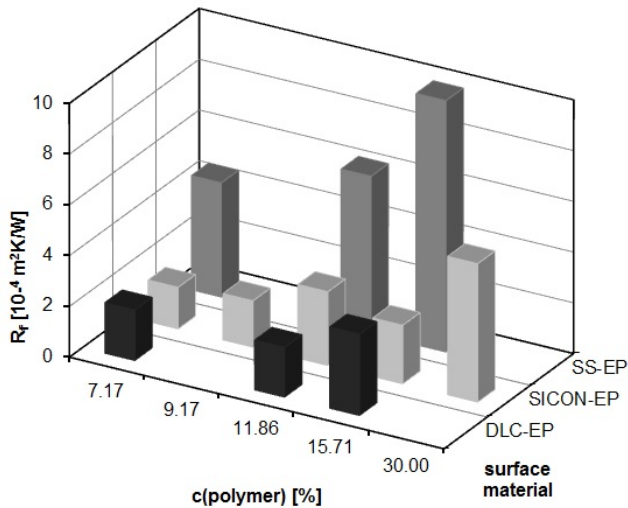


Fig. 12: Influence of the concentration of polymer on the thermal fouling resistance for electropolished surfaces. ($T_F = 50^\circ\text{C}$; $dq/dt = 3,4\text{kW/m}^2$ for SS-EP and $T_F = 50^\circ\text{C}$; $dq/dt = 5,1\text{kW/m}^2$ for DLC-EP. SICON-EP).

As there are numerous exceptions to all of these trends, the configurations of operational parameters are summarized in Table 1. In this study, all experiments, which delivered values for R_f^* of less than $2 \times 10^{-4} \text{ m}^2\text{K/W}$ were considered as best configurations. There are optimal configurations for almost the entire ranges of parameters, so this table can be used as a toolbox for process designers, who want to realize polymer processing. In these cases, the fouling tendency can rapidly increase when one of the parameter is shifted. This fact makes SICAN on electropolished and non-electropolished surfaces an interesting surface. All results on these surfaces delivers R_f^* values between 2 and $3.5 \times 10^{-4} \text{ m}^2\text{K/W}$. Compared to the entire pool of results in this study, the fouling behavior is quite low, even if experimental configurations do not appear in table 1. This can be seen in Fig. 13. The minimum values of R_f^* for SICAN and SICAN-EP coatings are higher than the minimum values for DLC, SICON or SS-EP plates. The maximum values of R_f^* for SICAN and SICAN-EP plates are lower than the maximum R_f^* value for any other plate.

Table 1. Configurations of operational parameters with the lowest thermal fouling resistance.

surface	c [%]	dq/dt [kW/m^2]	T [$^\circ\text{C}$]	$R_f [10^{-4} \text{ m}^2\text{K/W}]$
SS	7.2	3.4	40	1.85
SS	7.2	8.5	40	1.7
EP	11.9	1.7	55	0.75
EP	11.9	8.5	55	1.54
DLC	7.2	3.4	50	1.1
DLC	7.2	1.7	70	1.65
DLC	7.2	3.4	70	1.75
SICON®	7.2	5.1	55	1.79
SICON®	9.2	7.1	63.9	1.89
SICON®	11.9	5.1	70	1.17
SICON®	15.7	5.1	55	1.30
DLC-EP	7.2	5.1	50	1.99
DLC-EP	7.2	8.5	70	1.85
DLC-EP	9.2	5.1	70	1.27
SICAN-EP	7.2	8.5	50	1.73
SICON®-EP	7.2	5.1	55	1.63
SICON®-EP	7.2	8.5	50	1.78
SICON®-EP	9.2	5.1	70	1.98
SICON®-EP	9.2	5.1	50	1.92

Figure 13 shows the lowest determined thermal fouling resistance on a surface (indicated with a black bar) and the highest determined thermal fouling resistance (indicated with a grey bar). It can be observed that SICAN®, SS-EP, DLC, DLC-EP and SICON-EP can lead to a low fouling tendency, but with a broad range of R_f^* values with changing experimental parameters. The lowest range of values was obtained on SICAN and SICAN-EP surfaces. For a polymer processing plant that allows a broad range of operational conditions.

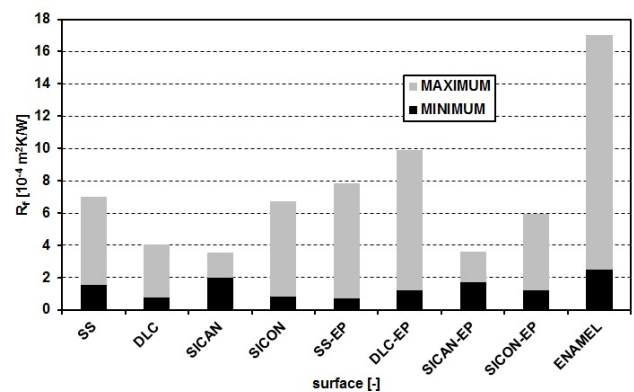


Fig. 13: Minimal and maximal values of the thermal fouling resistance for all investigated surfaces.

Fig. 14, 15 and 16 show micrographs of typical fouling layers. The most frequent structure of a polymer fouling layer is a crater like structure which is shown in Fig. 14. This structure was found in 80 % of the experiments. In many cases, larger craters contain smaller craters. The dependence of the size of the craters will be discussed later. As the temperature under the plate does not exceed 85 °C, these craters are not the result of an evaporation process. In 20 % of all experiments, other structures were obtained such as fiber like structures as shown in Fig. 15 or amorphous structures as shown in Fig. 16. A systematic dependency of the structure on the investigated operational parameters could not be observed so far.

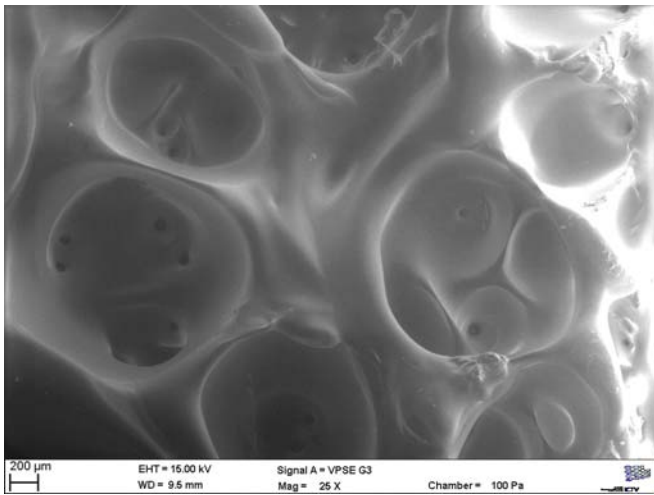


Fig. 14: SEM Picture of the fouling layer. ($T_f = 60\text{ °C}$, $c_{\text{polymer}} = 7.2\%$, heat flux density = 8.5 kW/m^2) on SICAN coated stainless steel.

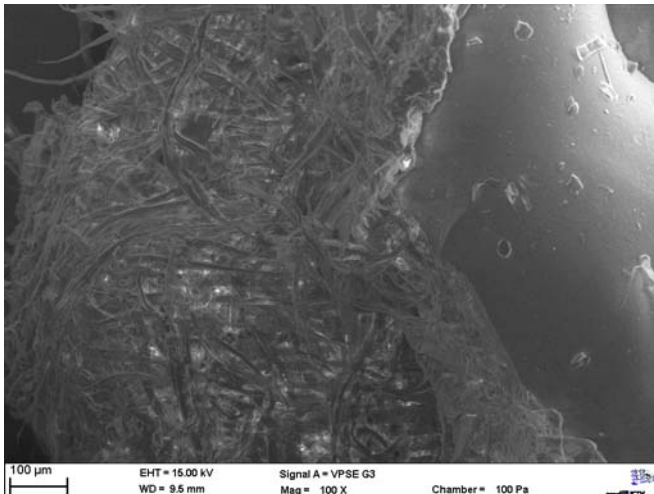


Fig. 15: SEM Picture of the fouling layer. ($T_f = 60\text{ °C}$, $c_{\text{polymer}} = 7.2\%$, heat flux density = 8.5 kW/m^2) on SICAN coated stainless steel.

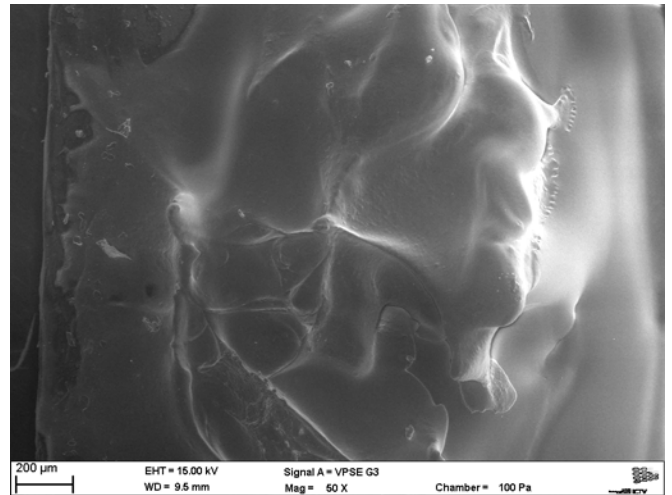


Fig. 16: SEM Picture of the fouling layer. ($T_f = 60\text{ °C}$, $c_{\text{polymer}} = 7.2\%$, heat flux density = 8.5 kW/m^2) on SICAN coated stainless steel.

As most of the fouling layers are crater structured, the diameter and the height of the craters were measured. The influence of the heat flux density on the diameter is shown in Fig. 17 and its influence on the height is shown in Fig. 18. The sizes were classified and the percentage of the size intervals is shown in the diagrams. The diameter and height increases with increasing heat flux density. The same trend could be observed with the other parameters: the diameter and height of the craters increases with increasing polymer concentration and temperature. As surface temperatures are below 90 °C in all of the experiments, the formation of bubbles can be excluded as reason for the crater structure. Currently, there are two possible explanations. It is possible that the polyols rearrange at higher temperatures and determine the shape of the remaining polymer. A second explanation might be physically solved gas. At increasing temperature, the gas might form bubbles. These bubbles can determine the size and shape of craters.

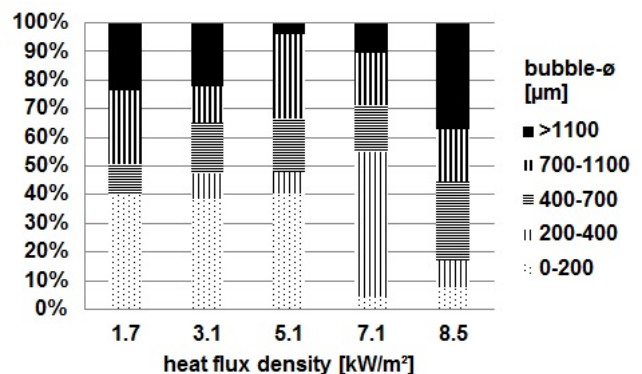


Fig. 17: Influence of the heat flux density in the diameter of the craters of the fouling layer.

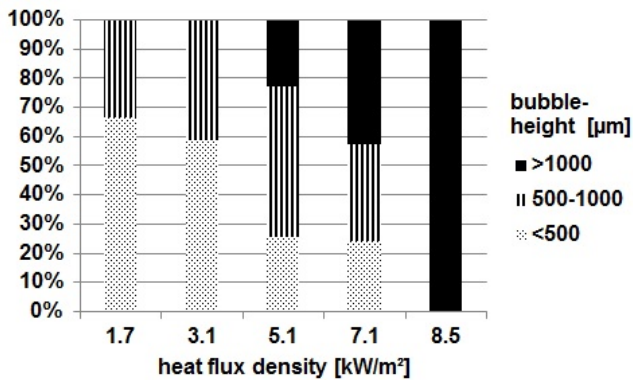


Fig. 18: Influence of the heat flux density on the height of the craters of the fouling layer.

On cooled surfaces, polymerfouling occurs, too. In contrast to the fouling behavior on heated surfaces, the fouling tendency is lower. Furthermore, the prerequisite for polymer fouling on cooled surfaces is a high concentration of polymer in the dispersion. In the present study, observable fouling occurs at polymer concentration of at least 30 %, see table 2. The first row of table 2 shows a reference experiment without cooling. Only in the experiments with at least 30 % of polymer, fouling was observed visually and could be determined by weighing. Fouling layers in cooled surfaces are very homogeneous, in contrast to the crater structures on fouling layers on heated surfaces, see Fig. 19.



Fig. 19: Fouling layer on a cooled surface of stainless steel caused by 55 wt-% polymer dispersion.

Table 2. Configurations of operational parameters with cooled surfaces.

surface	c [%]	T [°C]	m _f [g]
SS*	30	50	0.0379
SS	11.9	50	0.0093
SS	11.9	70	0.0348
SS	30	50	0.0530
SS	55	50	0.5244
DLC	11.9	50	0.0172
DLC	7.2	50	0.0097
DLC-EP	11.9	50	0.0103

CONCLUSIONS

In this study polymer fouling was investigated with a compound of industrial relevance. With heated and cooled plates and experiments in a batch vessel conditions which occur in polymerization and polymer processing steps were observed. Some trends of the influence of the key process parameters influence on the thermal fouling resistance could be found, which are not always consistent. Therefore, the best configurations were identified to deliver a toolbox of parameter configurations for those who practically design or operate polymer processing. In future, fouling experiments in a flow channel with cooled plates will be necessary. Further fouling experiments should also consider not just polymer but also polymerization fouling on cooled plates with an ongoing polymerization reaction. To validate the approach of reducing the fouling by surface modifications, the range of hydrophobicity/hydrophilicity of the surface material should be extended.

NOMENCLATURE

c	concentration of polymer, % of mass
k ₀	heat transfer coefficient of surface without fouling, W/m ² K
k	heat transfer coefficient of surface, W/m ² K
m _f	mass of fouling layer, g
OAc	acetate group
\dot{q}	heat flux density, kW/m ²
R	alkyl rest
R _f	thermal fouling resistance, m ² K/W
R _f [*]	thermal fouling resistance at the end of experiment, m ² K/W
S	surface, material or coating
SEM	scanning electron microscope
T	temperature, °C
T _f	bulk temperature, °C
t	time, s

REFERENCES

Bott, T.R., *Fouling of Heat Exchangers*, publ. Elsevier, Amsterdam, 1995.

Changani, S.D., Belmar-Beini, M.T., Fryer, P.J.; *Engineering and chemical factors associated with fouling and cleaning in milk processing*; Experimental Thermal and Fluid Science, 14, 392-406, 1997.

Characklis, W.G., Marshall, K. C.; *Biofilms*, John Wiley and Sons, New York, 1991

Epstein, N., *Fouling of Heat Exchangers*. In: Heat Exchangers; Theory and Practices, Eds. J. Taborek et. al., Hemisphere Publishing Corp., London, 1983

Melo, L.F., Bott, T.R.; *Biofouling in water systems*, Experimental and Thermal Fluid Science, 14, 375-381, 1997

Geddert, T., Augustin, W., Bialuch, I., Scholl, S., Extending the induction period of crystallization fouling through surface coating, Müller-Steinhagen et al., Heat Exchanger Fouling & Cleaning VII, Berkeley Electronic Press, 2008

Geddert, T., *Einfluss von Oberflächenmodifikationen auf die Induktionszeit beim Kristallisationsfouling*, Dissertation, TU Braunschweig, 2009.

Müller Steinhagen, H.: *Verschmutzung von Wärmeübertragerflächen*. In: VDI Wärmeatlas, Springer, Berlin, 2006.

VDI Wärmeatlas, Berechnungsblätter für den Wärmeübergang, Springer, Berlin, 2006.